CHEMISTRY
A European Journal

A Journal of ChemPubSoc Europe

Title: Tailored band gaps in sulphur and nitrogen containing porous donor-acceptor polymers (SNPs)

Authors: Dana Schwarz, Yaroslav S. Kochergin, Amitava Acharja, Arun Ichangi, Maksym V. Opanasenko, Jiří Čejka, Uwe Lappan, Pal Arki, Junjie He, Johannes Schmidt, Petr Nachtigall, Arne Thomas, and Michael Janus Bojdys

To be cited as: *Chem. Eur. J.* 10.1002/chem.201703332

Link to VoR: http://dx.doi.org/10.1002/chem.201703332

Supported by ACES

WILEY-VCH

Tailored band gaps in sulphur and nitrogen containing porous donor-acceptor polymers (SNPs)

Dana Schwarz,[a] Yaroslav S. Kochergin,[a] Amitava Acharja,[b] Arun Ichangi,[a],[c] Maksym V. Opanasenko,[d] Jiří Čejka,[d] Uwe Lappan,[e] Pal Arki,[f] Junjie He,[g] Johannes Schmidt,[b] Petr Nachtigall,[g] Arne Thomas,[b] Michael J. Bojdys*[a],[c]

This manuscript is dedicated to Pierre Kuhn – a pioneer of triazine-based frameworks – who sadly passed away in May 2017.

Abstract: Donor-acceptor dyads hold the key to tuning of electrochemical properties and enhanced mobility of charge carriers, yet their incorporation into a heterogeneous polymer network proves difficulty due to the fundamentally different chemistry of the donor- and acceptor-subunits. We present a family of sulphur and nitrogen containing porous polymers (SNPs) that are obtained *via* Sonogashira-Hagihara cross-coupling and that combine electron-withdrawing triazine (C_3N_3) and electron donating, sulphur-containing linkers. Choice of building blocks and synthetic conditions determines the optical band gap (from 1.67 to 2.58 eV) and nanoscale ordering of these microporous materials with BET surface areas of up to 545 $m^2\ g^{-1}$ and CO_2 capacities up to 1.56 $mmol\ g^{-1}$. Our results highlight the advantages of the modular design of SNPs, and we report one of the highest photocatalytic hydrogen evolution rates for a cross-linked polymer without Pt co-catalyst (194 $\mu mol\ h^{-1}\ g^{-1}$).

Microporous polymer materials have attracted enormous attention in the past decade due to their applications in gas storage, heterogeneous catalysis, chemical separation and organic electronics.[1] Recently, covalent triazine-based frameworks (CTFs) have been prepared *via* trimerisation of aromatic nitriles under ionothermal-[2] and Brønsted acid-catalysed conditions.[3] The linking-motif of CTFs – the aromatic triazine (C_3N_3) ring – acts as an electron acceptor, and it has been explored as an electron-withdrawing group in conjugated microporous polymers (CMPs).[4] Incorporation of electron donors – such as sulphur and carbon containing ring-systems[5] – into electron accepting CTFs is desirable, since it is associated with an improved performance in photovoltaics, nonlinear optics, and (opto-)electronics,[6] and since it enables us to modulate the redox potential range of the resulting materials with relative ease.[7]

We propose a synthetic strategy to join the interesting properties of triazine- and sulphur-containing linkers – including tetrathiafulvalene (TTF), dihydrothienothiophene, and bithiophene – into one family of sulphur and nitrogen containing porous polymers (SNPs). Hence, we have opted for a synthetic route to link triazine-containing tectons using a palladium-catalysed Sonogashira-Hagihara cross-coupling reaction.[1a] We obtain three covalent SNPs (**SNP-TTF**, **SNP-1**, and **SNP-2**) and two polymers with naphthyl- and biphenyl-bridges (**NP-1** and **NP-2**) as yellow to brown powders in good to excellent yields (80 to 90%) (Scheme 1 and SI). Here, **NP-1** is an interesting reference compound, since it is structurally analogous to – yet more defined and more ordered than – a previously reported CMP (TCMP-5) by Cooper et al.[4n] (Note: the synthetic protocol for TCMP-5 uses an excess of C_3/C_2–symmetric building blocks of 1 to 2.25 instead of the ideal 1 to 1.5 molar ratio.)

The composition of the SNPs is confirmed by IR spectroscopy, elemental analysis (EA), and X-ray photoelectron spectroscopy (XPS) (see SI). All materials show a signal at 172 ppm indicative of triazine ring-carbons in ^{13}C cross-polarisation magic-angle spinning (CP/MAS) NMR spectroscopy (Figure 1). The peaks between 124 and 142 ppm are assigned to the sp^2-hybridised carbons in phenyl groups and within sulphur containing tectons. The peaks between 88 and 99 ppm are sp-hybridised -C≡C- sites.

All of the obtained networks are mainly amorphous by powder X-ray diffraction (PXRD) (Figure S19). However, networks **NP-1**, **NP-2**, and **SNP-1** show weak first-order peaks visible at 2.3°, 1.2°, and 1.2° 2θ, respectively (Figure S20). These peaks correlate with primary reflexes expected for the large, hexagonal unit cells of the fully condensed materials (predicted *via* DFT as a =b = 43.924 Å for **SNP-TTF**, 41.163 Å for **SNP-1**, 43.894 Å for **SNP-2**, 45.148 Å for **NP-1**, and 41.831 Å for **NP-2**, Table S13). Distances between aromatic struts in the polymer backbone can be deduced from the broad peaks visible between 20 and 25° 2θ (4.4 to 3.6 Å) that are common for layered and interdigitating, aromatic systems like other COFs.[2b]

---

[a] Dr. D. Schwarz, Y. S. Kochergin, A. Ichangi, Dr. M. J. Bojdys
Charles University, Department of Organic Chemistry
Hlavova 8 128 43 Prague 2, Czech Republic
E-mail: m.j.bojdys.02@cantab.net
[b] Dr. A. Acharjya, Dr. J. Schmidt, Prof. Dr. A. Thomas
Department of Functional Materials
Technical University Berlin
Hardenbergstr. 40, 10623 Berlin, Germany
[c] A. Ichangi, Dr. J. Tarábek, Dr. M. J. Bojdys
Institute of Organic Chemistry and Biochemistry of the CAS
Flemingovo nam. 2, 166 10 Prague 6, Czech Republic
[d] Dr. M. V. Opanasenko, Prof. Dr. J. Čejka
Heyrovsky Institute for Physical Chemistry
Academy of Science Czech Republic
Dolejškova 3, 182 23 Prague 8, Czech Republic
[e] Dr. U. Lappan
Leibniz-Institut fuer Polymerforschung Dresden e.V.
Hohe Str. 6, 01069 Dresden, Germany
[f] Dr. P. Arki
Technical University Bergakademie Freiberg
Gustav Zeuner Str. 3, 09599 Freiberg, Germany
[g] Dr. J. He, Prof. Dr. P. Nachtigall
Charles University, Department of Physical and Macromolecular Chemistry, Hlavova 8, 128 43 Prague 2, Czech Republic

Supporting information for this article is given *via* a link at the end of the document.

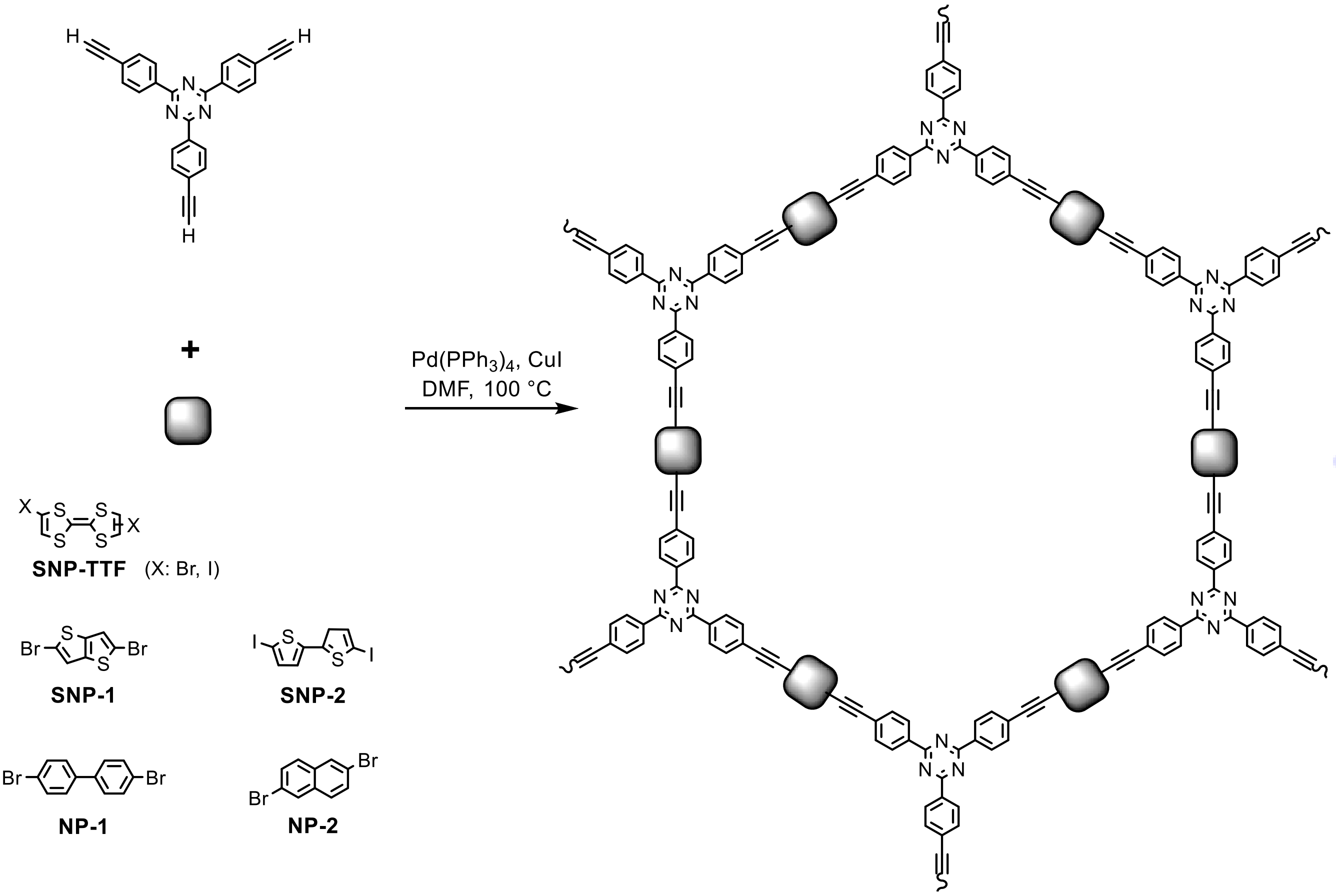

Scheme 1. Synthetic route to SNPs. *C*$_3$-symmetric 2,4,6-tris(4-ethynylphenyl)-1,3,5-triazine is coupled with a *C*$_2$-symmetric bridge such as: dihalo-2,2'-bi(1,3-dithiolylidene) to yield **SNP-TTF**, 2,5-dibromo-3a,6a-dihydrothieno[3,2-b]thiophene to yield **SNP-1**, 5,5'-diiodo-2,2'-bithiophene to yield **SNP-2**, 4,4'-dibromo-1,1'-biphenyl to yield **NP-1**, and 2,6-dibromonaphthalene to yield **NP-1**.

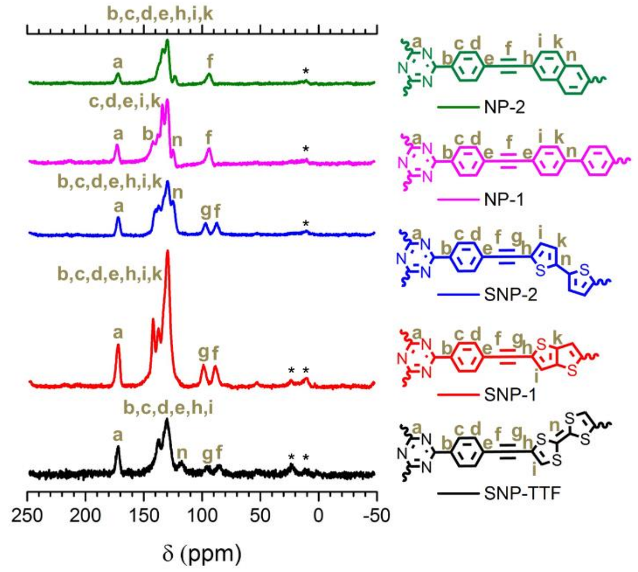

Figure 1. ^{13}C CP-MAS ssNMR spectra of SNPs from top to bottom **NP-2** (in green), **NP-1** (in magenta), **SNP-2** (in blue), **SNP-1** (in red), and **SNP-TTF** (in black). The triazine carbon signal (marked a) appears at 172 ppm, and the quaternary diyene carbons (marked f and g) at ~88-99 ppm. Phenyl peaks are marked as b, c, d, and e. Spinning sidebands are denoted with an asterisk (*).

Networks **SNP-TTF**, **SNP-2**, and **NP-2** show pronounced Moiré fringes in their transmission electron microscopy (TEM) images, and the corresponding selected area electron diffraction (SAED) patterns indicate a polycrystalline arrangement of thin layers (Figure 2).[8]

Nitrogen (N_2) sorption isotherms at 77 K for all networks show accessible Brunauer–Emmett–Teller (BET) surface areas between 273 and 545 m^2 g^{-1} and a pronounced hysteresis which is common for microporous conjugated polymers (Figure 3 a, Table 1).[9] Notably, the two networks derived from structural ambiguous synthons – **SNP-TTF** (273 m^2 g^{-1}; cis/trans isomerism of its halogenated TTF-synthon), and **SNP-2** (370 m^2 g^{-1}; flexible bithiophene bridge) – also have the lowest accessible surface areas. In contrast, networks with strictly *C*$_2$ symmetric bridges show overall larger surface areas up to 545 m^2 g^{-1} for **SNP-1** (Table 1).

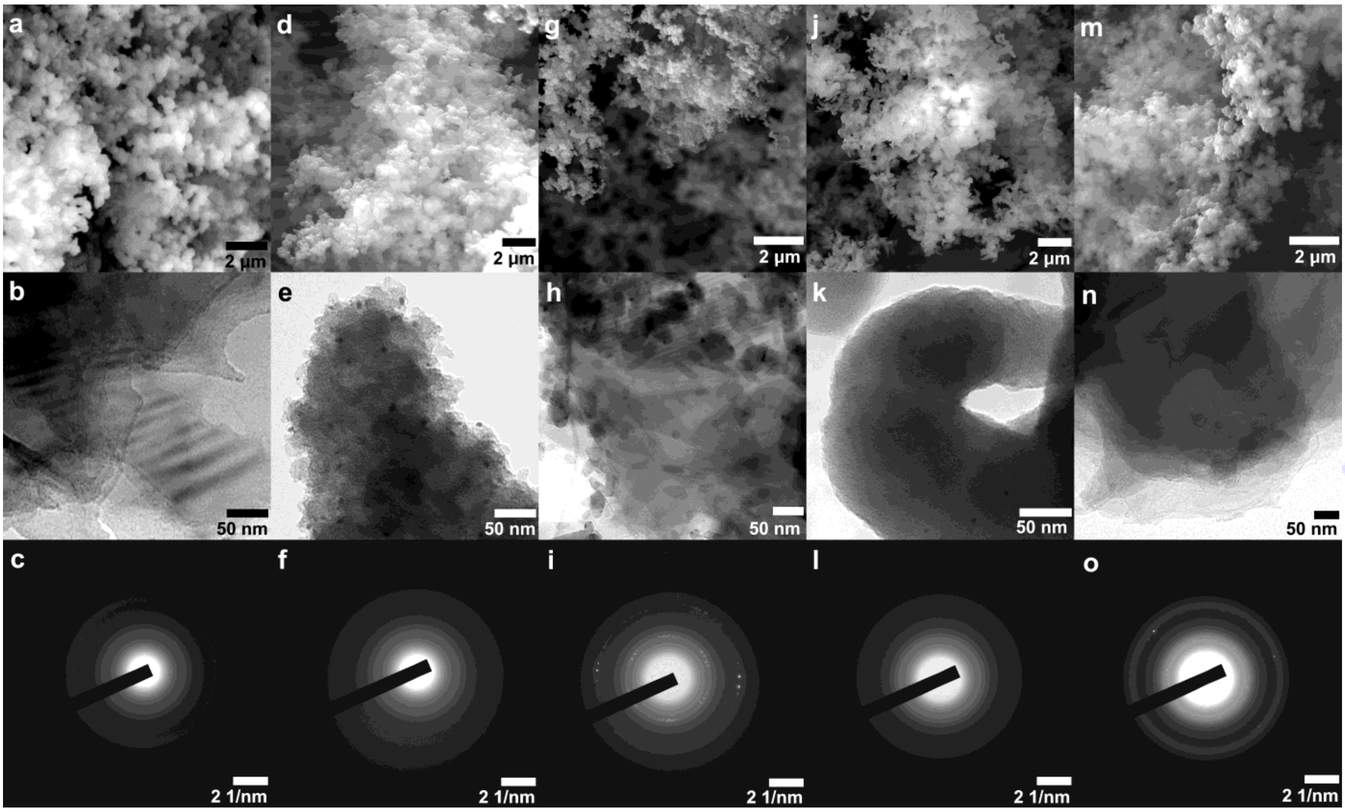

Figure 2. Electron microscopic investigation of SNPs. SEM (top), TEM (centre), and SAED (bottom) images for: a-c) **SNP-TTF**, d-f) **SNP-1**, g-i) **SNP-2**, j-l) **NP-1**, and m-o) **NP-2**. b, h and n) Networks **SNP-TTF**, **SNP-2**, and **NP-2** show Moiré fringes in TEM images indicative of overlapping, ordered layers. c, i, and o) The same networks show concentric rings in the electron diffraction that are indicative of polycrystalline domains.

It is noteworthy, that these values are among the highest of all hitherto reported sulphur and nitrogen containing microporous polymers (Table S14).[9c],[10] Pore size distribution (PSD) analysis shows a broad range of pore diameters between 1 and 10 nm which correlates well with the large pore windows and the complex stacking arrangements expected for these networks (Figure 3 b).

Table 1. Porosity parameters of SNPs.

sample	S_{BET} (m^2 g^{-1})[a]	PV (cm^3 g^{-1})[b]	MPV (cm^3 g^{-1}) [c	CO_2 uptake (mmol g^{-1}) [d]
SNP-TTF	273	0.20	0.04	1.52
SNP-1	545	0.32	0.21	1.48
SNP-2	370	0.33	0.09	1.27
NP-1	469	0.32	0.17	1.56
NP-2	502	0.39	0.09	1.20

[a] surface area calculated from N_2 adsorption isotherm using BET equation. [b] pore volume (PV) calculated from N_2 uptake at $p/p_0 = 0.95$. [c] micro pore volume (MPV) calculated from N_2 uptake at $p/p_0 = 0.10$. [d] CO_2 uptake calculated for 273 K and 1 bar.

Due to the large accessible pore volume and the overall conjugation of the organic donor-acceptor (D-A) backbone, SNPs and NPs yield themselves particularly well to iodine (I_2) sorption from the gas phase and from a solution of I_2 in ethanol (see SI).[9a] Sorption from the gas phase was the more efficient uptake process and is discussed in the following. We found that iodine is dispersed homogeneously throughout the pores without aggregating into observable crystals (*via* PXRD, Figure S19), nor does it chemically alter the networks (*via* IR spectroscopy, Figure S23). Previous reports claim a beneficial effect of sulphur content on iodine loading.[11] We find, however, that overall uptake of iodine correlates significantly with overall accessible surface area (Figure S3). **SNP-1** has the highest surface area and takes up the highest amount of iodine (with 63.4 wt% and 545 m^2 g^{-1}). Sulphur-free **NP-1** and **NP-2** are ideal examples to corroborate this hypothesis, and they follow the same trend. High heteroatom-content is believed to be beneficial for the physisorption of carbon dioxide (CO_2) in CMPs.[3] However, for our SNPs and NPs we have found no systematic correlation of CO_2 sorption with either accessible surface area nor with S, N-content. All polymers show very similar, moderate CO_2 capacities at 273 K and 1 bar between 1.56 mmol g^{-1} for **NP-1**, and 1.20 mmol g^{-1} for **NP-2** (Table 1, and Figure S25).

Diffuse reflectance UV/Vis spectra show discernible absorption edges starting at ~550 nm for **NP-2** to ~770 nm for **SNP-TTF** (Figure 4 a). According to the Kubelka-Munk function, that corresponds to direct band gap values of 2.58 eV for **NP-2**, and 1.6 eV for **SNP-TTF** (Figure S22). Iodine loading into the networks is accompanied by darkening of the materials and a red-shift of the absorption edge. We propose that this optical effect is a consequence of p-type doping induced by iodine.

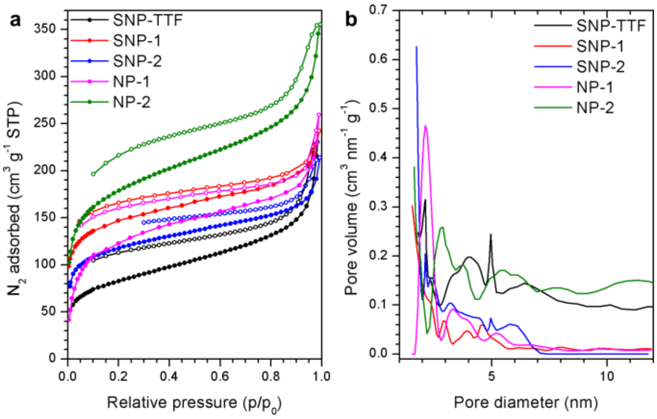

Figure 3. a) Nitrogen (N_2) de-/sorption isotherms measured at 77 K for **SNP-TTF** (in black), **SNP-1** (in red), **SNP-2** (in blue), **NP-1** (in magenta), and **NP-2** (in green). Data points in the adsorption and desorption branch of the isotherms are indicated by filled and empty circles, respectively. b) Pore size distribution (PSD) analysis for the adsorption branch calculated using cylind. oxide surface (for SNP-TTF, SNP-2), quenched solid state density functional theory (QS-DFT) cylind. pores (for SNP-1, NP-1), and C-slit non-local density functional theory (NL-DFT) (for NP-2).

To this end, we examine the electron paramagnetic resonance (EPR) spectra of neat (S)NPs before and after iodine loading (Figure S26 and S27). The EPR signal of the neat networks is centred at g = 2.006 for **SNP-TTF** (linewidth of~2 mT) and at g = 2.003 (linewidth of ~0.6-0.9 mT) for all other SNPs and NPs. The linewidth and shape of the EPR signal is comparable to that of undoped films of conductive polymers such as polyaniline and poly(methyl methacrylate) (g values of ~2.003, and linewidths of 0.4-0.8 mT), and we expect that the spins are delocalised over several rings of the aromatic (S)NP backbone.[12] Iodine loading broadens the linewidth by a factor of up to 1.5. This is indicative of more localised spins presumably due to real charge-transfer between network and dopant, and the formation of iodide (I_x^-, typically I_3^-) species.[5a, c] Indeed, undoped **SNP-TTF** shows two separate maxima and minima peaks in the EPR that are a consequence of the spin-coupling of mixed-valence states in the TTF linker.[5c, 13] This double-peak merges into one signal after positive charge-localisation on the TTF moiety and the formation of iodide.[5a, c] All samples – with the exception of **NP-1** – feature an up to four-fold increase in signal intensity after doping which correlates with an equivalent increase in concentration of paramagnetic species. Indeed, the resistivity of doped materials decreases by a factor of up to 400 (see SI). However, results of these tests are inconclusive and vary widely due to the powder-like sample-morphology.

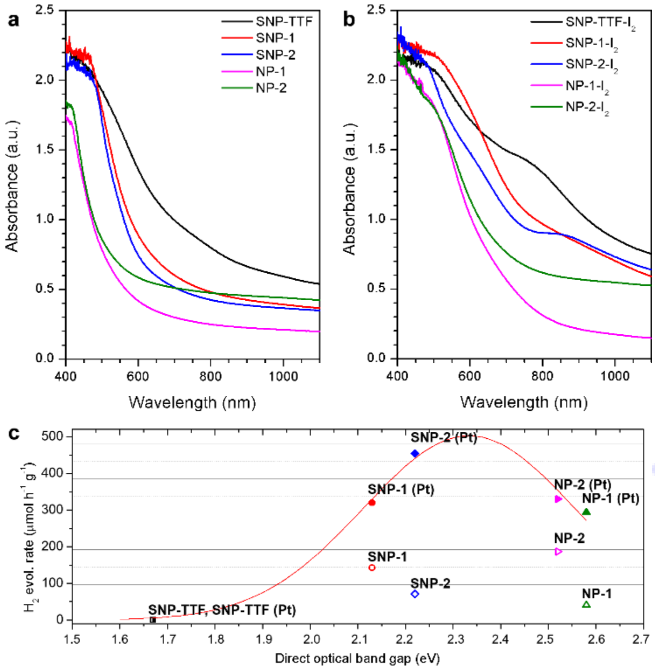

Figure 4. a) Solid-state UV/Vis diffuse-reflectance spectra of pristine and b) iodine loaded SNPs and NPs showing **SNP-TTF** (in black), **SNP-1** (in red), **SNP-2** (in blue), **NP-1** (in magenta), and **NP-2** (in green). c) Hydrogen evolution rates of SNPs and NPs under visible light (395 nm cut-off filter) correlated with the direct optical band gap. Each measurement was performed in a water:acetonitrile (1:1) mixture using triethanolamine (TEOA) as sacrificial agent with 3 wt% platinum (Pt) (filled symbols) and without Pt co-catalyst (empty symbols). Hydrogen evolution rates of (S)NPs with Pt co-catalyst peak at an optical band gap of 2.2 to 2.3 eV, and tail off at the extremes (red line).

More interestingly, all networks – with the exception of **SNP-TTF** – evolve hydrogen from water under visible light (395 nm cut-off filter) with and without platinum (Pt) as co-catalyst (Figure 4 c).[14] Although, there are some benchmark photocatalysts – like heptazine based polymers (1600 µmol h^{-1} g^{-1}),[15] and azine based COFs (1703 µmol h^{-1} g^{-1})[16] – that outperform (S)NPs, none of the previously reported materials show any photocatalytic activity without a noble-metal co-catalyst. It is noteworthy, that no added co-catalyst does not necessarily equate to a truly "metal-free” photocatalysis. Yu et al. investigated the photocatalytic activity of a series of S- and N-containing polymers achieving hydrogen evolution rates of up to 106.9 µmol h^{-1} without the addition of a co-catalyst.[17] However, the report states a residual palladium (Pd) content from the Sonogashira-Hagihara cross-coupling of between 0.73 and 2.13 wt% that may facilitate the hydrogen evolution reaction.[18] In our SNPs and NPs, we detect residual Pd content between 0.13 and 0.02 wt% – one order of magnitude lower than in previous reports – *via* inductively coupled plasma optical emission spectrometry (ICP-OES) (Table S5), energy-dispersive X-ray (EDX) spectroscopy (Table S6), and XPS (Table S8). **SNP-2** performs best with 3 wt% Pt co-catalyst at 472 µmol h^{-1} g^{-1}, while **NP-2** achieves 194 µmol h^{-1} g^{-1} without Pt co-catalyst. This one of the highest reported values and an improvement over amorphous CMPs that achieved up to 120 µmol h^{-1} g^{-1} of evolved hydrogen without additional co-catalyst.[19] Peak hydrogen evolution rates are reached around 2.2 to 2.3 eV when co-catalyst is used to reduce the over-potential (Figure 4 c), with a drop to zero for **SNP-TTF**. This trend has been observed for dark-coloured, carbon-only photocatalysts, too,[20] and is a consequence of fast, non-radiative electron-hole recombination.

In conclusion, we have synthesised a family of sulphur and nitrogen containing polymers (SNPs) that feature an open, pore-structure and incorporate an intriguing donor-acceptor motif: electron rich, sulphur-containing bridges and electron poor triazines. (S)NP chemistry is highly modular enabling us to systematically vary the donor-acceptor backbone and its optical properties, and hence, to optimise the photocatalytic hydrogen evolution activity of these materials. In particular, we report one of the highest hydrogen evolution rates of 194 µmol h^{-1} g^{-1} without the addition of expensive, noble-metal co-catalyst. The overall π-conjugated backbone of SNPs and NPs yields itself to post-synthetic tuning – as demonstrated here *via* p-doping – and opens up the prospect of further, rational band gap tuning *via* electrochemical means.

Acknowledgements

We thank Dr. Nikolai Makukhin for discussions, Šárka Pšondrová is acknowledged for IR, Dr. Simona Hybelbauerova for her support in solid-state NMR, Dr. Jiri Rybacek and Dr. Martin Racek for their support in SEM and EDX, Stanislava Matejkova.is acknowledged for ICP-OES, Jaroslava Hnilickova is acknowledged for EA and Christina Eichenauer is acknowledged for BET and TGA. M.J.B. thanks the European Research Council (ERC) for funding under the Starting Grant scheme (BEGMAT – 678462). M.J.B., J.C. and P.N. further acknowledge the Charles University Centre of Advanced Materials (CUCAM) (OP VVV Excellent Research Teams, project number CZ.02.1.01/0.0/0.0/15_003/0000417).

Keywords: conjugated microporous polymers • donor-acceptor dyads • triazine • photocatalysis

[1] a) J.-X. Jiang, F. Su, A. Trewin, C. D. Wood, N. L. Campbell, H. Niu, C. Dickinson, A. Y. Ganin, M. J. Rosseinsky, Y. Z. Khimyak and A. I. Cooper, *Angew. Chem., Int. Ed.* **2007**, *46*, 8574-8578; b) J. M. H. Thomas and A. Trewin, *J. Phys. Chem. C* **2014**, *118*, 19712-19722; c) J. Germain, J. M. J. Fréchet and F. Svec, *Small* **2009**, *5*, 1098-1111; d) N. B. McKeown and P. M. Budd, *Chem. Soc. Rev.* **2006**, *35*, 675-683; e) P. Kaur, J. T. Hupp and S. T. Nguyen, *ACS Catal.* **2011**, *1*, 819-835; f) N. Chaoui, M. Trunk, R. Dawson, J. Schmidt and A. Thomas, *Chem. Soc. Rev.* **2017**, *46*, 3302-3321.

[2] a) M. J. Bojdys, J. Jeromenok, A. Thomas and M. Antonietti, *Adv. Mater.* **2010**, *22*, 2202-2205; b) P. Kuhn, M. Antonietti and A. Thomas, *Angew. Chem., Int. Ed.* **2008**, *47*, 3450-3453.

[3] S. Ren, M. J. Bojdys, R. Dawson, A. Laybourn, Y. Z. Khimyak, D. J. Adams and A. I. Cooper, *Adv. Mater.* **2012**, *24*, 2357-2361.

[4] a) R. Fink, C. Frenz, M. Thelakkat and H.-W. Schmidt, *Macromolecules* **1997**, *30*, 8177-8181; b) H. Meier, E. Karpuk and H. Christof Holst, *Eur. J. Org. Chem.* **2006**, *2006*, 2609-2617; c) I. Nenner and G. J. Schulz, *J. Chem. Phys.* **1975**, *62*, 1747-1758; d) K. M. Omer, S.-Y. Ku, Y.-C. Chen, K.-T. Wong and A. J. Bard, *J. Am. Chem. Soc.* **2010**, *132*, 10944-10952; e) Y. Oumi, Y. Kakinaga, T. Kodaira, T. Teranishi and T. Sano, *J. Mater. Chem.* **2003**, *13*, 181-185; f) S. Ren, Q. Fang, F. Yu and D. Bu, *J. Polym. Sci., Part A: Polym. Chem.* **2005**, *43*, 6554-6561; g) S. Ren, D. Zeng, H. Zhong, Y. Wang, S. Qian and Q. Fang, *J. Phys. Chem. B* **2010**, *114*, 10374-10383; h) T. Yamamoto, S. Watanabe, H. Fukumoto, M. Sato and T. Tanaka, *Macromol. Rapid Commun.* **2006**, *27*, 317-321; i) L. Zou, Y. Fu, X. Yan, X. Chen and J. Qin, *J. Polym. Sci., Part A: Polym. Chem.* **2008**, *46*, 702-712; j) L. Zou, Y. Liu, N. Ma, E. Macoas, J. M. G. Martinho, M. Pettersson, X. Chen and J. Qin, *Phys. Chem. Chem. Phys.* **2011**, *13*, 8838-8846; k) L. Zou, Z. Liu, X. Yan, Y. Liu, Y. Fu, J. Liu, Z. Huang, X. Chen and J. Qin, *Eur. J. Org. Chem.* **2009**, *2009*, 5587-5593; l) F. Pop, F. Riobe, S. Seifert, T. Cauchy, J. Ding, N. Dupont, A. Hauser, M. Koch and N. Avarvari, *Inorg. Chem.* **2013**, *52*, 5023-5034; m) J. C. Ren, R. Q. Zhang, Z. J. Ding and M. A. Van Hove, *RSC Adv.* **2014**, *4*, 64577-64582; n) S. Ren, R. Dawson, A. Laybourn, J.-x. Jiang, Y. Khimyak, D. J. Adams and A. I. Cooper, *Polym. Chem.* **2012**, *3*, 928-934; o) M. Trunk, A. Herrmann, H. Bildirir, A. Yassin, J. Schmidt and A. Thomas, *Chem. - Eur. J.* **2016**, *22*, 7179-7183.

[5] a) H. Ding, Y. Li, H. Hu, Y. Sun, J. Wang, C. Wang, C. Wang, G. Zhang, B. Wang, W. Xu and D. Zhang, *Chem. - Eur. J.* **2014**, *20*, 14614-14618; b) T. C. Narayan, T. Miyakai, S. Seki and M. Dincă, *J. Am. Chem. Soc.* **2012**, *134*, 12932-12935; c) H. Bildirir, J. P. Paraknowitsch and A. Thomas, *Chem. - Eur. J.* **2014**, *20*, 9543-9548; d) R. S. Sprick, B. Bonillo, R. Clowes, P. Guiglion, N. J. Brownbill, B. J. Slater, F. Blanc, M. A. Zwijnenburg, D. J. Adams and A. I. Cooper, *Angew. Chem., Int. Ed.* **2016**, *128*, 1824-1828.

[6] M. R. Bryce, *Adv. Mater.* **1999**, *11*, 11-23.

[7] D. Lorcy and N. Bellec, *Chem. Rev.* **2004**, *104*, 5185-5202.

[8] M. Valamanesh, C. Langlois, D. Alloyeau, E. Lacaze and C. Ricolleau, *Ultramicroscopy* **2011**, *111*, 149-154.

[9] a) J. Jeromenok and J. Weber, *Langmuir* **2013**, *29*, 12982-12989; b) Y. Liao, J. Weber, B. M. Mills, Z. Ren and C. F. J. Faul, *Macromolecules* **2016**, *49*, 6322-6333; c) S. Ren, R. Dawson, D. J. Adams and A. I. Cooper, *Polym. Chem.* **2013**, *4*, 5585-5590.

[10] H. Bohra, S. Y. Tan, J. Shao, C. Yang, A. Efrem, Y. Zhao and M. Wang, *Polymer Chemistry* **2016**, *7*, 6413-6421.

[11] X. Qian, Z. Q. Zhu, H. X. Sun, F. Ren, P. Mu, W. D. Liang, L. H. Chen and A. Li, *ACS Appl. Mater. Interfaces* **2016**, *8*, 21063-21069.

[12] K. H. Wu, Y. S. Lai, C. C. Shih, G. P. Wang and C. C. Yang, *Polym. Compos.* **2008**, *29*, 902-905.

[13] M. Di Valentin, A. Bisol, G. Agostini, P. A. Liddell, G. Kodis, A. L. Moore, T. A. Moore, D. Gust and D. Carbonera, *J. Phys. Chem. B* **2005**, *109*, 14401-14409.

[14] a) J. Kiwi and M. Gratzel, *Nature* **1979**, *281*, 657-658; b) D. J. Martin, K. Qiu, S. A. Shevlin, A. D. Handoko, X. Chen, Z. Guo and J. Tang, *Angew. Chem., Int. Ed.* **2014**, *53*, 9240-9245.

[15] K. Kailasam, M. B. Mesch, L. Möhlmann, M. Baar, S. Blechert, M. Schwarze, M. Schröder, R. Schomäcker, J. Senker and A. Thomas, *Energy Technology* **2016**, *4*, 744-750.

[16] K. Schwinghammer, B. Tuffy, M. B. Mesch, E. Wirnhier, C. Martineau, F. Taulelle, W. Schnick, J. Senker and B. V. Lotsch, *Angew. Chem., Int. Ed.* **2013**, *52*, 2435-2439.

[17] L. Li, W.-y. Lo, Z. Cai, N. Zhang and L. Yu, *Macromolecules* **2016**, *49*, 6903-6909.

[18] Y. Wang, X. Wang and M. Antonietti, *Angew. Chem., Int. Ed.* **2012**, *51*, 68-89.

[19] R. S. Sprick, B. Bonillo, M. Sachs, R. Clowes, J. R. Durrant, D. J. Adams and A. I. Cooper, *Chem. Commun.* **2016**, *52*, 10008-10011.

[20] R. S. Sprick, J.-X. Jiang, B. Bonillo, S. Ren, T. Ratvijitvech, P. Guiglion, M. A. Zwijnenburg, D. J. Adams and A. I. Cooper, *J. Am. Chem. Soc.* **2015**, *137*, 3265-3270.

Entry for the Table of Contents

COMMUNICATION

Sulphur and nitrogen containing porous polymers (SNPs) combine two key-features for heterogeneous photocatalysts, namely an open pore-structure, and a modular, π-conjugated backbone. We demonstrate how the electronic and optical properties of these photoactive materials can be tuned *via* the choice of building blocks and *via* post-synthetic doping.

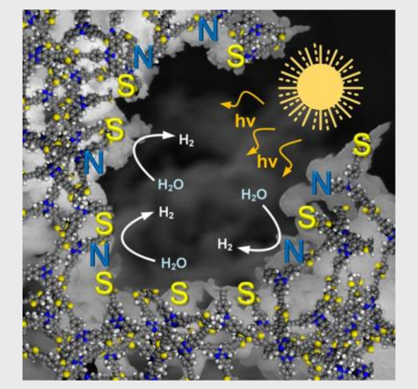

*Dana Schwarz, Yaroslav S. Kochergin, Amitava Acharja, Arun Ichangi, Maksym V. Opanasenko, Jiří Čejka, Uwe Lappan, Pal Arki, Junjie He, Johannes Schmidt, Petr Nachtigall, Arne Thomas, Michael J. Bojdys**

Page No. – Page No.

Sulphur and nitrogen containing porous donor-acceptor polymers (SNPs)